

LITERATURE CITED

1. N. F. Krasnov, V. N. Koshevoi, and V. T. Kalugin, Aerodynamics of Separated Flows [in Russian], Moscow (1988).
2. V. A. Grigor'ev and V. M. Zorin, eds., Heat and Mass Transfer. Thermotechnical Experiment: Handbook [in Russian], Moscow (1982).
3. L. M. Khritov and A. I. Khudyakov, Tr. TsIAM, No. 676, 1-7, Moscow (1975).
4. E. U. Repik, Yu. P. Sosedko, and L. G. Shikhov, Tr. TsAGI, No. 1599, 42-53, Moscow (1974).
5. V. F. Pavlenko, Power Plants with Thrust Vector Rotation in Flight [in Russian], Moscow (1987).

INVESTIGATION OF THE HEAT TRANSFER LAWS IN A
THREE-DIMENSIONAL VISCOUS SHOCK LAYER ON BLUNT
BODIES AT ANGLE OF ATTACK AND SIDESLIP

A. I. Borodin and S. V. Peigin

UDC 533.6.011

The authors analyze the results of numerical solution of the equations of the three-dimensional thin viscous shock layer over triaxial ellipsoids of different shapes in a flow of supersonic viscous gas, with no symmetry planes.

In many applied tasks one needs to investigate the basic laws of heat transfer in three-dimensional flow of a supersonic viscous heat-conducting gas over blunt bodies of complex shape, over a wide range of Reynolds numbers. The thin viscous shock layer theory, first proposed in [1], is widely used to solve these problems. Being comparatively simple mathematically (a problem of parabolic type) this theory allows one to eliminate a number of defects present in the widely-used boundary layer theory. On the one hand, in shock layer theory one need not divide the entire flow region into individual sublayers, because the appropriate equations are uniformly applicable in the entire perturbed flow region from the shock wave to the body surface. On the other hand the shock layer equations describe the flow correctly, asymptotically, over a substantially wider range of change of Reynolds number, from small through medium to large [2].

However, the shock layer model possesses a number of limitations, associated in particular, with the fact that the use of a simplified momentum equation along the normal leads to the appearance on the surface of a convex body of zero pressure lines (separation lines), beyond which the solution cannot be continued.

On the whole, however, as is confirmed by analysis of numerous comparisons of solutions of shock layer equations with experimental data and with computations on a more complete formulation (see the review in [3]), the thin viscous shock layer model has good accuracy over quite a wide region of the forward surface of blunt bodies for which the shock layer thickness is small compared with a characteristic body dimension, and the surface pressure p_w is on the same order as the stagnation point value p_0 ($p_w/p_0 \approx 0.05-0.1$).

Taking into account the above limitations, in this study we have solved the three-dimensional thin shock layer equations in their region of application in the case of flow over triaxial ellipsoids of different shapes at angle of attack and sideslip. We have analyzed the influence of body shape, Reynolds number, and the other governing parameters of the problem on the basic heat transfer laws. Previously the thin shock layer equations have been solved for different special cases of three-dimensional flows in [4-11]. In [4, 5] the authors investigated flow over delta wings of infinite size at angles of attack and sideslip, in [6] the authors investigated flow over rotating axisymmetric bodies at zero angle

Scientific Research Institute for Applied Mathematics and Mechanics, Tomsk State University. Translated from *Inzhenerno-Fizicheskii Zhurnal*, Vol. 58, No. 2, pp 200-206, February, 1990. Original article submitted October 31, 1988.

of attack, and in [7] the authors investigated flow in the vicinity of a stagnation point with double curvature. In [8, 9] an approximate approach was proposed to determine the longitudinal pressure gradients on the lateral surface, thus closing the problem outside the stagnation point, for flow in the symmetry plane of blunt bodies; in [10] this was proposed for flow at angle of attack over bodies with two planes of symmetry; and in [11] for flow with no planes of symmetry. There are also papers where the laws of heat transfer over blunt bodies with a permeable surface in flow at angle of attack and sideslip, have been studied on the three-dimensional boundary layer theory, applicable at large Reynolds number [12, 13].

We consider flow in a three-dimensional thin viscous shock layer on blunt bodies washed at angle of attack and sideslip by a supersonic stream of viscous, heat-conducting gas. In a curvilinear coordinate system (ξ, η, ζ) (ζ is reckoned along the normal to the body, and ξ, η are chosen on the surface analogously as in [13]) the initial equations have the following dimensionless form [2]:

$$\begin{aligned} & \frac{\partial}{\partial \xi} \left(\rho u \sqrt{\frac{a}{a_{11}}} \right) + \frac{\partial}{\partial \eta} \left(\rho w \sqrt{\frac{a}{a_{22}}} \right) + \frac{\partial}{\partial \zeta} (\rho v \sqrt{a}) = 0, \\ & \rho (Du + A_1^1 u^2 + A_2^1 u w + A_3^1 w^2) = - \frac{2\varepsilon \sqrt{a_{11}}}{1 + \varepsilon} \left(a^{11} \frac{\partial p}{\partial \xi} + a^{12} \frac{\partial p}{\partial \eta} \right) + \\ & \quad + \frac{\partial}{\partial \zeta} \left(\frac{\mu}{K} \frac{\partial u}{\partial \zeta} \right), \quad \rho (Dw + A_1^2 u^2 + A_2^2 u w + A_3^2 w^2) = \\ & \quad = - \frac{2\varepsilon \sqrt{a_{22}}}{1 + \varepsilon} \left(a^{21} \frac{\partial p}{\partial \xi} + a^{22} \frac{\partial p}{\partial \eta} \right) + \frac{\partial}{\partial \zeta} \left(\frac{\mu}{K} \frac{\partial w}{\partial \zeta} \right), \quad (1) \\ & \rho DT = \frac{2\varepsilon}{1 + \varepsilon} D^0 p + \frac{\partial}{\partial \zeta} \left(\frac{\mu}{\sigma K} \frac{\partial T}{\partial \zeta} \right) + \frac{\mu}{K} \left[\left(\frac{\partial u}{\partial \zeta} \right)^2 + \left(\frac{\partial w}{\partial \zeta} \right)^2 + \right. \\ & \quad \left. + 2 \cos \psi \frac{\partial u}{\partial \zeta} \frac{\partial w}{\partial \zeta} \right], \quad \frac{\partial p}{\partial \zeta} = -0.5(1 + \varepsilon) \rho (A_1^3 u^2 + A_2^3 u w + A_3^3 w^2), \\ & p = \rho T, \quad K = \varepsilon \text{Re}, \quad \mu = T^\omega, \quad T_0 = T_\infty (\gamma - 1) M_\infty^2, \\ & \varepsilon = \frac{\gamma - 1}{\gamma + 1}, \quad \text{Re} = \frac{\rho_\infty V_\infty R}{\mu(T_0)}, \quad D \equiv D^0 + v \frac{\partial}{\partial \zeta}, \\ & D^0 \equiv \frac{u}{\sqrt{a_{11}}} \frac{\partial}{\partial \xi} + \frac{w}{\sqrt{a_{22}}} \frac{\partial}{\partial \eta}, \quad \cos \psi = \frac{a_{12}}{\sqrt{a_{11} a_{22}}}. \end{aligned}$$

The system (1) is solved with the no slip and no penetration conditions on the body surface

$$\zeta = 0: u = w = v = 0, \quad T = T_w(\xi, \eta) \quad (2)$$

and the generalized Rankine-Hugoniot conditions at the shock wave

$$\begin{aligned} & \zeta = \zeta_s(\xi, \eta): \rho(v - D^0 \zeta_s) = v_\infty, \quad p = \frac{1 + \varepsilon}{2} v_\infty^2, \\ & \frac{\mu}{K} \frac{\partial u}{\partial \zeta} = v_\infty (u - u_\infty), \quad \frac{\mu}{K} \frac{\partial w}{\partial \zeta} = v_\infty (w - w_\infty), \quad (3) \\ & \frac{\mu}{\sigma K} \frac{\partial T}{\partial \zeta} = v_\infty \{ T - 0.5 [v_\infty^2 + (u - u_\infty)^2 + (w - w_\infty)^2 + 2 \cos \psi (u - u_\infty)(w - w_\infty)] \}. \end{aligned}$$

Analysis shows that the stagnation point $\xi = 0$ is a singular point of the system of differential equations (1). In addition, for $\xi = 0$ the system of coordinates (ξ, η) used on the body surface is degenerate. Therefore in the numerical solution of the boundary problem (1)-(3) we convert to the new dependent and independent variables, allowing us to isolate the given special features:

$$\xi^* = \xi, \quad \eta^* = \eta, \quad \zeta^* = \frac{1}{\Delta} \int_0^\xi \rho d\zeta, \quad \Delta = \int_0^{\zeta_s} \rho d\zeta, \quad (4)$$

$$u^* = \frac{u}{u_\infty}, \quad w^* = \frac{w}{\xi}, \quad \theta = \frac{2T}{v_\infty^2}, \quad P_1 = \frac{1}{\xi} \frac{\partial p}{\partial \xi}, \quad P_2 = \frac{1}{\xi^2} \frac{\partial p}{\partial \eta}.$$

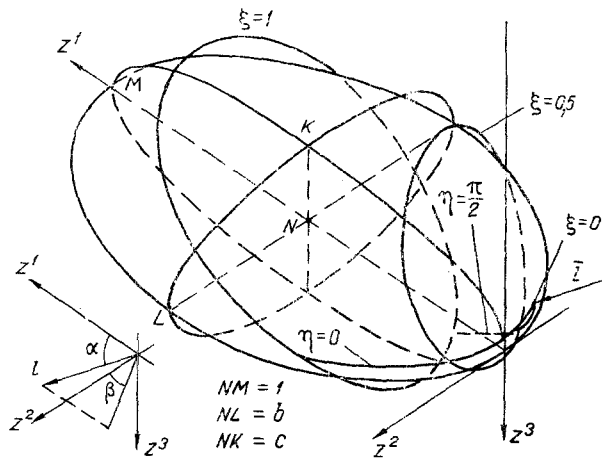


Fig. 1. General geometry of the flow.

After converting to the variables (4) we solve numerically the system of equations and boundary conditions thus obtained. Here, because of the choice of a coordinate system on the surface, the solution has a number of special features. Firstly, since η varies in the range $0 \leq \eta \leq 2\pi$, and all the coefficients in the original equations are periodic functions of η , then in the solution we took into account the periodicity of all the desired functions with respect to the coordinate η . In addition, because of the degeneracy of the coordinate system (ξ, η) at the point $\xi = 0$, to obtain the solution in the vicinity of the stagnation point in a manner analogous to that of [13], we used a nondegenerate curvilinear, locally Cartesian coordinate system whose axes coincided with the body surface normal, and with the direction of the principal normal cross sections of the body at the stagnation point.

A finite-difference solution was found using a scheme having approximation order $O(\Delta\zeta)^4 + O(\Delta\xi) + O(\Delta\eta)^2$, which is a generalization of the scheme of [14]. The derivatives with respect to ξ were computed using backward differences, and derivatives with respect to η were approximated by central differences. For stability of the numerical algorithm, the value of $\Delta(\xi, \eta)$, describing the shock wave standoff distance, was determined by the cyclic marching method [15].

As an example we examined the flow at an angle of attack α and sideslip angle β over triaxial ellipsoids of different shapes. The geometrical flow scheme is shown in Fig. 1. In a rectangular coordinate system (z^1, z^2, z^3) the equation of the ellipsoid surface had the form

$$(z^1 - 1)^2 + \left(\frac{z^2}{b}\right)^2 + \left(\frac{z^3}{c}\right)^2 = 1. \quad (5)$$

In this case the connection between the coordinate system (ξ, η) on the ellipsoid surface and the original Cartesian system $\{z^1\}$ can be written in explicit form:

$$\begin{aligned} z^1 &= 1 - A \cos(m\xi) - E^{-1} \sin(m\xi) (AB \cos \eta + C \sin \eta), \\ z^2 &= b [E \cos \eta \sin(m\xi) - B \cos(m\xi)], \\ z^3 &= -c [C \cos(m\xi) + E^{-1} \sin(m\xi) (BC \cos \eta - A \sin \eta)], \\ D &= \{1 + b^2 \operatorname{tg}^2 \alpha + \operatorname{tg}^2 \beta (1 + c^2 \operatorname{tg}^2 \alpha)\}^{1/2}, \quad A = (D \cos \beta)^{-1}, \\ B &= bD^{-1} \operatorname{tg} \alpha, \quad C = cD^{-1} \operatorname{tg} \alpha \operatorname{tg} \beta, \quad E = (A^2 + C^2)^{1/2}. \end{aligned} \quad (6)$$

The function $m = m(\eta)$ was chosen from the condition that the normal to the ellipsoid surface on the line $\xi = 1$ be perpendicular to the unit vector $l(\cos \alpha, \sin \alpha \cos \beta, \sin \alpha \sin \beta)$, giving the direction of the incident flow:

$$m(\eta) = \begin{cases} \pi - \operatorname{arctg} \frac{N}{|F|}, & F < 0, \\ \frac{\pi}{2}, & F = 0, \\ \operatorname{arctg} \frac{N}{F}, & F > 0, \end{cases}$$

$$\begin{aligned}
F &= M \cos \eta + L \sin \eta, \quad N = A \cos \alpha + Bb^{-1} \sin \alpha \cos \beta + Cc^{-1} \sin \alpha \sin \beta, \\
M &= Eb^{-1} \sin \alpha \cos \beta - ABE^{-1} \cos \alpha - BC(Ec)^{-1} \sin \alpha \sin \beta, \\
L &= E^{-1}(Ac^{-1} \sin \alpha \sin \beta - C \cos \alpha).
\end{aligned}
\tag{7}$$

The governing parameters of the problem were varied in the following ranges:

$$0.3 \leq b \leq 3, \quad 0.3 \leq c \leq 3, \quad 0 \leq \alpha \leq \frac{\pi}{2}, \quad 0 \leq \beta \leq \frac{\pi}{4}, \tag{8}$$

$$\varepsilon = 0.1, \quad \omega = 0.5, \quad 10^2 \leq Re \leq 5 \cdot 10^5, \quad 0.05 \leq \theta_w = \text{const} \leq 0.25.$$

The average computing time on the BESM-6 computer for one item on a $15 \times 45 \times 15$ mesh (in the directions ξ , η , ζ , respectively) was 1.5 h.

During the computations we determined the components of the velocity vector, the temperature and the pressure across the shock layer, the shock wave standoff distance, and also the coefficients of friction and heat transfer on the body surface, for which the expressions have the following form:

$$\begin{aligned}
q &= \lambda \frac{\partial T}{\partial \zeta} \frac{2 \sqrt{Re}}{\rho_\infty V_\infty^3}, \quad \tau_\xi = \mu \frac{\partial}{\partial \zeta} \left(\frac{u}{u_\infty} \right) \frac{\sqrt{Re}}{\rho_\infty V_\infty^2}, \\
\tau_\eta &= \mu \frac{\partial}{\partial \zeta} \left(\frac{w}{\xi} \right) \frac{\sqrt{Re}}{\rho_\infty V_\infty^2}, \quad c_q = \frac{q(\xi, \eta)}{q(0, \eta)}, \\
c_\xi &= \frac{\tau_\xi(\xi, \eta)}{\tau_\xi(0, \eta)}, \quad c_\eta = \frac{\tau_\eta(\xi, \eta)}{\tau_\eta(0, \eta)}.
\end{aligned}
\tag{9}$$

We turn now to the matter of the influence of the body shape and angles of attack and sideslip on the heat flux distribution along the surface. For $\alpha = \beta = 0$ there are two symmetry planes in the flow, in which the distribution c_q has local extrema. As is shown in Fig. 2a, the nature of these extrema depends to a great extent on b and c . For $b = 0.7$, $c = 0.3$ the heat flux falls off monotonically along both planes of symmetry, and the stagnation point is a point of local maximum of c_q . For $b = 2$, $c = 3$ the opposite picture is observed: as the distance from the stagnation point increases along both planes of symmetry the heat flux increases, so that at the stagnation point the distribution of c_q has a minimum. For the intermediate case of $b = 2$, $c = 0.5$ the point $\xi = 0$ is a saddle point in the c_q distribution, since in the plane z^1Oz^2 the heat flux increases with increasing distance from the stagnation point, and it falls off in the plane z^1Oz^3 . As is shown by analysis, this kind of dependence of the c_q distribution in the vicinity of the stagnation point on the ellipsoid shape has quite a clear physical meaning.

Actually, it is clear that the heat flux to the body surface falls off with reduction of temperature at the outer edge of the boundary layer, and, on the other hand, increases with increase of the energy released within the shock layer, due to effects of viscous dis-

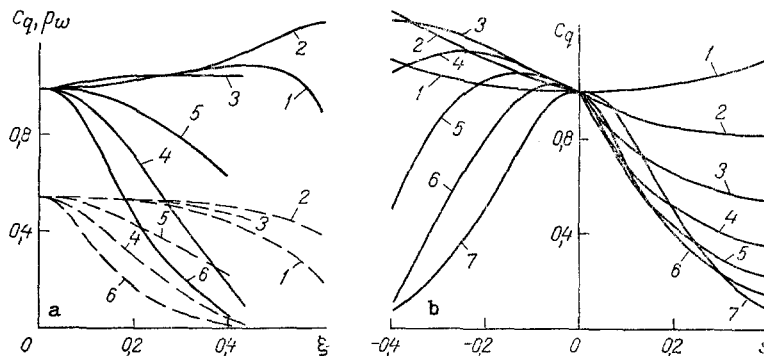


Fig. 2. Distributions of c_q and p_w in the planes of symmetry of ellipsoids of different shapes for $\beta = 0$, $Re = 5 \cdot 10^4$, $\theta_w = 0.15$ and various angles of attack: a) $\alpha = 0$, $\eta = 0$, (1, 3, 5), $\eta = 90^\circ$ (2, 4, 6), $b = 2$, $c = 3$ (1, 2); $b = 2$, $c = 0.5$ (3, 4); $b = 0.7$, $c = 0.3$ (5, 6); b) $b = 2$, $c = 3$, $\alpha = 0, 15, 30, 45, 60, 75, 90^\circ$ - 1-7.

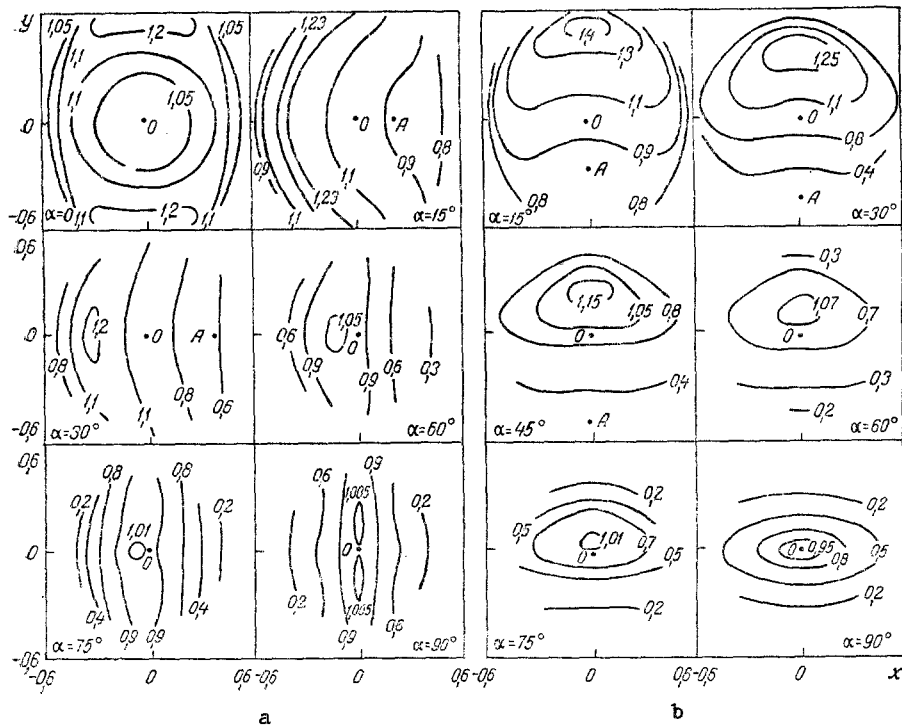


Fig. 3. Dependence of isolines of c_q along the surface of the ellipsoids on the angle of attack for $\beta = 0$, $Re = 5 \cdot 10^4$, $\theta_w = 0.15$: a) $b = 2$, $c = 3$; b) $b = 3$, $c = 2$.

sipation. The temperature at the outer edge of the boundary layer is proportional to the pressure p_w on the body surface, while the intensity of viscous dissipation is inversely proportional to the radius of longitudinal curvature of the ellipsoid shape in the plane of its symmetry. For $b < 1$, $c < 1$, as can be seen in Fig. 2a, the quantity p_w (broken lines) falls off quite rapidly with increasing distance from the stagnation point, while the radii of the longitudinal curvature increase monotonically with increase of ξ , so that in this case the stagnation point is a point of local maximum of c_q . For $b > 1$, $c > 1$ the decrease of p_w is less significant, but the radii of curvature become monotonically decreasing functions of ξ , as a result of which, for $b \gtrsim 1.5$, $c \gtrsim 1.5$ the effects of the viscous dissipation begin to prevail over the factors causing a decrease of heat flux, and for a given b and c the stagnation point becomes a point of local minimum of c_q . It is important to note that, as the results of the computations show, the law noted above in the distributions of c_q along the planes of symmetry of the ellipsoids in flow at zero angle of attack remains valid over a wide range of the Reynolds number and for large Re this effect is more pronounced.

For flow over a body at angle of attack with $\beta = 0$ there is only one plane of symmetry in the flow. The characteristic form of the distribution of c_q with respect to the coordinate s ($s = \xi$ for $\eta = 0$ and $s = -\xi$ for $\eta = \pi$) in the plane of symmetry for different angles of attack is shown in Fig. 2b. It can be seen that for the given case ($b = 3$, $c = 2$) the stagnation point for $\alpha = 0$ is a point of local minimum. For small α this minimum is moved from the stagnation point in the direction of increased radius of longitudinal curvature of the ellipsoid profile in the plane of its symmetry, and in the region where this radius decreases, there is a local maximum in the c_q distribution. With further increase of the angle of attack this minimum vanishes, while the local maximum decreases in magnitude and moves towards the stagnation point, so that for $\alpha = 90^\circ$, when there is a second plane of symmetry in the flow, the stagnation point becomes a point of local maximum of c_q for the given plane of symmetry.

On the whole the computations have shown that even when the flow has a single plane of symmetry, the picture of the heat flux distribution along the body surface has quite a complex form, and, depending on the ellipsoid shape and the angle of attack, it may be qualitatively different in nature.

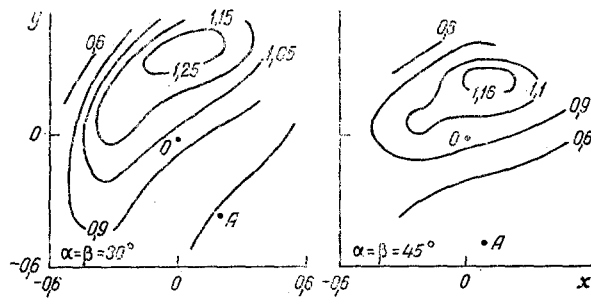


Fig. 4. Form of isolines of c_q for $b = 2$, $c = 3$, $Re = 5 \cdot 10^4$, $\theta_w = 0.15$ for non-zero angle of attack and sideslip.

This is easily seen in Fig. 3, which shows the evolution of isolines of the heat flux c_q in the plane of the variables (x, y) ($x = \xi \cos \eta$, $y = \xi \sin \eta$) (Fig. 3a) and $x = \xi \sin \eta$, $y = -\xi \cos \eta$ (Fig. 3b) as a function of the angle of attack for $b = 2$, $c = 3$ and $b = 3$, $c = 2$. The point 0 in these figures corresponds to the stagnation point, and the point A corresponds to the "nose" of the ellipsoid $z^1 = z^2 = z^3 = 0$. It can be seen that, depending on the ratios between b and c , the stagnation point, at which for $\alpha = \beta = 0$ the heat flux had a local minimum, as the angle of attack increases up to 90 deg can become either a saddle point in the c_q distribution (Fig. 3a), or a point of local maximum of the heat flux (Fig. 3b).

In conclusion we present a typical form of the isolines of heat flux on the surface for the general case of flow over an ellipsoid at nonzero angle of attack and sideslip (Fig. 4). It can be seen that there is no symmetry in the c_q distribution, and the corresponding picture is complex and three-dimensional.

NOTATION

ξR , ηR , ζR , dimensioned curvilinear coordinates, fixed in the wetted surface of the body; R , characteristic linear dimension of the problem; uV_∞ , wV_∞ , $vV_\infty \epsilon$, physical components of the velocity vector in the directions ξ , η , ζ , respectively; $\rho \rho_\infty \epsilon^{-1}$, $\rho_\infty V_\infty^2 (\gamma + 1) p / \gamma$, $T_0 T$, $\mu_0 \mu$, the density pressure, temperature and viscosity; σ , Prandtl number; w , exponent in the dependence of viscosity on temperature; Re , Reynolds number; M_∞ , Mach number; $a_{\alpha\beta}$, covariant components of the basic metric tensor; $a = a_{11} a_{22} - a_{12}^2$; $\Delta = \Delta(\xi, \eta)$ a quantity characterizing the shock wave standoff distance; A'_{jk} coefficients depending in a known way on the components of the metric tensors $a_{\alpha\beta}$ and the coordinates ξ , η on the body surface; α , angle of attack; β , sideslip angle; $\gamma = c_p / c_v$, adiabatic exponent. The subscripts ∞ , w , s , and 0 refer, respectively, to the parameters of the incident flow, on the body surface, on the shock wave, and at the stagnation point of the incident flow.

LITERATURE CITED

1. H. K. Cheng, Proc. Heat Transfer and Fluid Mech Inst., Stanford Press (1961).
2. É. A. Gershbein, Hypersonic Three-Dimensional Flow with Physical and Chemical Transformation [in Russian], Moscow (1981), pp. 29-51.
3. É. A. Gershbein, S. V. Peigin, and G. A. Tirkii, Itogi Nauki Tekh. Mekh. Zhidk. Gaza, 19, 3-85 (1985).
4. I. G. Brykina, and É. A. Gershbein, Izv. Akad. Nauk SSSR, Mekh. Zhidk. Gaza, No. 2, 91-102 (1979).
5. É. A. Gershbein, V. S. Shchelin, and S. A. Yunitskii, Izv. Akad. Nauk SSSR, Mekh. Zhidk. Gaza, No. 4, 104-108 (1984).
6. É. A. Gershbein, and S. V. Peigin, Izv. Akad. Nauk SSSR, Mekh. Zhidk. Gaza, No. 6, 27-37 (1986).
7. É. A. Gershbein, and S. A. Yunitskii, Zh. Prikl. Mat. Mekh., 43, No. 5, 817-828 (1979).
8. R. R. Eaton, and P. C. Kaestner, AIAA Paper No. 134 (1973).
9. É. A. Gershbein, and S. A. Yunitskii, Zh. Prikl. Mat. Mekh., 48, No. 5, 768-775 (1984).
10. É. A. Gershbein, V. S. Shchelin, and S. A. Yunitskii, Hypersonic Three-Dimensional Flow with Physical and Chemical Transformations [in Russian], Moscow (1981), pp. 72-92.
11. É. A. Gershbein, V. G. Krupa, and V. S. Shchelin, Zh. Prikl. Mat. Mekh., 50, No. 1, 110-118 (1986).

12. A. I. Borodin and S. V. Peigin, *Teplofiz. Vysok. Temp.*, 25, No. 3, 509-515 (1987).
13. A. I. Borodin and S. V. Peigin, *Inzh-Fiz. Zh.*, 53, No. 3, 365-372 (1987).
14. I. V. Petukhov, *Numerical Methods of Solving Differential and Integral Equations and Quadrature Formulas* [in Russian], Moscow (1964), pp. 304-325.
15. A. A. Samarskii and E. S. Nikolaev, *Methods of Solving Mesh Equations* [in Russian], Moscow (1978).

RANDOM MOTION OF SOLID PARTICLES AND ENERGY

DISSIPATION IN TWO-PHASE FLOW

L. I. Krupnik, P. V. Ovsienko,
V. N. Oleinik, and V. G. Ainshtein

UDC 532.529.5

We obtain equations describing the fluctuations and energy loss of particle collisions in two-phase flow from the experimental velocity distribution functions.

The random motion of solid particles in a turbulent gas flow is one of the deciding factors in the formation of hydrodynamic structures in two-phase flow and it significantly affects the intensity of transport processes [1]. The mechanism of the generation of random motion is usually [2-5] explained in terms of the time and spatial scales of turbulence in the carrier medium and collisions between the particles and the walls of the channel.

Theoretical studies [4, 5] have shown that as the particle relaxation time increases, the degree to which the particles are drawn into the fluctuating motion of the gas decreases and approaches zero in the case when the phases slip past one another with their average velocities. This type of two-phase motion takes place in the transport of hydraulically large particles of sizes $1 \cdot 10^{-4}$ - $3 \cdot 10^{-3}$ m in chemical engineering processes such as heterogeneous catalysis, gasification of coal, adsorption, dehydration, sorting, and so on.

The mathematical description of the motion of solid particles with their collisions taken into account [6, 7] leads to equations containing the stress tensor in the solid phase and the flux vector of the fluctuating motion of the solid particles as unknowns. As shown in [6], these quantities can be expressed explicitly in terms of the macroscopic parameters of the two-phase flow in the framework of the statistical theory of dispersed systems with the help of the position and velocity distribution functions of the solid particles.

There is no information available in the literature on the parameters of random motion in two-phase flow in the presence of collisions between the solid particles. This situation has stimulated the work described in the present paper.

We carried out a systematic experimental study of the distribution functions of the longitudinal $P(u_x)$ and transverse $P(u_y)$ components of the instantaneous velocities of glass balls of diameters $d = 113 \pm 9 \mu\text{m}$ and $d = 1.18 \text{ mm}$. The measurements were done by the contact method [8], in which signals can be detected from a single collision of a solid particle against the sensitive area of the detector. With the help of an AI-256-6 pulse analyzer, we obtained data on the normal component of the amplitude of the collision impulse, the time duration of the collision, the time interval between collisions, and the flux density of particles at different points in a cross section of the channel. The study was performed on the stabilized section of the motion in a vertical pipe of diameter $D = 2R = 50 \text{ mm}$. The velocity of the medium (air) was varied between 5 and 23 m/sec. The input-output ratio of solid particles in the flow reached 25 kg·h/(kg·h). Before taking measurements in the pipe, we first calibrated the detectors by fixing the number of the channel of the pulse analyzer receiving a signal from a particle of known size, and moving with a known velocity and contacting the sensitive element of the detector at a known angle of incidence.

State Research and Design Institute of Methanol and Products of Organic Synthesis, Severodonetsk. Translated from *Inzhenerno-Fizicheskii Zhurnal*, Vol. 58, No. 2, pp. 207-213, February, 1990. Original article submitted November 14, 1988.